UC Santa Barbara

UC Santa Barbara Previously Published Works

Title

Scanning transmission electron microscopy of gate stacks with HfO2 dielectrics and TiN electrodes

Permalink

https://escholarship.org/uc/item/6rf7c5q0

Journal

Applied Physics Letters, 87

Authors

Agustin, Melody P.
Fonseca, Leo R. C.
Hooker, Jacob C.
et al.

Publication Date

2005

Peer reviewed

eScholarship.org Powered by the California Digital Library
University of California

Scanning transmission electron microscopy of gate stacks with HfO_2 dielectrics and TiN electrodes

Melody P. Agustin

Materials Department, University of California, Santa Barbara, CA 93106-5050

Leonardo R. C. Fonseca

Freescale Semiconductores Brasil Ltda, Jaguariúna 13820-000, Brazil

Jacob C. Hooker

CMOS Module Integration, Philips Research Leuven, B-3001 Leuven, Belgium

Susanne Stemmer[a)]

Materials Department, University of California, Santa Barbara, CA 93106-5050

[a)] Electronic mail: stemmer@mrl.ucsb.edu

ABSTRACT

High-angle annular dark-field (HAADF) imaging and electron energy-loss spectroscopy (EELS) in scanning transmission electron microscopy were used to investigate HfO_2 gate dielectrics grown by atomic layer deposition on Si substrates, and their interfaces with TiN electrodes and silicon, as a function of annealing temperature. Annealing at high temperatures (900 °C) caused significant roughening of both bottom (substrate) and top (electrode) interface. At the bottom interface, HAADF images showed clusters of Hf atoms that protruded into the interfacial SiO_2 layer. Low-loss EELS established that even crystalline HfO_2 films exposed to relative high temperatures (700 °C) exhibited significant differences in their electronic structure relative to bulk HfO_2. Further annealing caused the electronic structure to more closely resemble that of bulk HfO_2, with the most significant change due to annealing with the TiN electrode.

Continued scaling of feature sizes in complementary metal-oxide-semiconductor (CMOS) devices will require the replacement of SiO_2 with gate dielectrics that have a higher dielectric constant (k), such as HfO_2. In addition, the heavily doped polycrystalline silicon gate electrode may have to be replaced with metal electrodes. Midgap gate electrode metals, such as TiN, are being extensively investigated [1-4]. The metal/dielectric and the dielectric/Si interface determine the CMOS device performance, including channel mobility and threshold voltage. To date, the chemistry and structure of these new interfaces remain poorly understood. For example, the precise chemistry of SiO_2-like interfacial layers formed between ZrO_2 or HfO_2 gate dielectrics and the Si substrate interface under oxidizing deposition conditions is still under debate. Electrical measurements show that the dielectric constant of these interfacial layers is greater than that of pure, bulk SiO_2 and it has been suggested that the interfacial layer is substoichiometric SiO_2 or a metal silicate [5-7]. Recent medium energy ion-scattering and electron energy-loss spectroscopy (EELS) studies found no evidence for silicate formation [8,9]. At the HfO_2/TiN interface, intermixing has been reported by some authors [2], whereas others report a thermally stable interface but with significant roughening [4].

The goal of this paper is an improved understanding of the structure and bonding in HfO_2 layers and their interfaces with the Si substrate and TiN electrodes as a function of annealing temperature. We use scanning transmission electron microscopy (STEM) based techniques, in particular high-angle annular dark-field (HAADF) imaging and EELS. As the signal at low energy losses is significantly delocalized, relatively thick HfO_2 films (~ 13 nm) were investigated to allow low-loss EELS to be recorded from the film without the influence from adjacent layers.

HfO_2 gate dielectrics were grown on *n*-type Si substrates (cleaned using the IMEC clean [10]) by atomic layer deposition (ALD) using alternating cycles of $HfCl_4$ and H_2O with N_2 carrier gas. A post-deposition anneal in O_2 at 700 °C for 60 seconds was carried out. 20 nm thick TiN capping layers were deposited by ALD ($TiCl_4$ and NH_3 at 350 °C) followed by another 20 nm of TiN grown by DC sputtering. These samples will be referred to as "as-deposited". Selected samples were exposed to rapid thermal anneals (RTA) in N_2 ambient for 30 s at 700 °C, 800 °C, and 900 °C, respectively.

TEM samples were prepared by standard sample preparation techniques with ion milling using 3.3 kV Ar ions as the final step. A monoclinic HfO_2 powder (99.9% purity with Zr < 50 ppm, Alfa Aesar) was used as a reference sample for EELS. Conventional high-resolution transmission electron microscopy (HRTEM), HAADF imaging and EELS were performed using a field-emission TEM (Tecnai F30U, Cs = 0.52 mm) operated at 300 kV. The probe size for EELS and HAADF was about 2 – 3 Å. EELS spectra were recoded using a Gatan Enfina 1000 spectrometer. The energy resolution (full-width at half-maximum of the zero-loss peak) was about 0.85 – 0.90 eV. Core-loss EELS spectra of N K-, Ti $L_{2,3}$- and O K-edge were also recorded.

HRTEM and HAADF showed that HfO_2 and TiN were polycrystalline in all samples. The HfO_2 grain sizes were larger than the film thickness even in the as-deposited sample (note that this sample was exposed to a 700 °C anneal). Figure 1 shows HAADF images of the 800 °C and the 900 °C annealed gate stack, respectively. For thin samples, the intensity in the HAADF images is approximately proportional to the atomic number Z^2, so that the HfO_2 layer appeared bright in these images, whereas the thin (1.3-1.5 nm) interfacial SiO_2-like layer appeared dark. Layer thicknesses were determined from inflection points of first derivatives of intensity line

profiles across the HAADF images [11]. The HfO_2 film thickness in the gate stacks annealed up to 800 °C was about 13.5 nm, while the HfO_2 film thickness in the 900 °C gate stack was ~ 12 nm, indicating some densification. Furthermore, roughening of the interfaces with TiN and SiO_2 is observed at 900 °C [Fig, 1(b)], which made it more difficult to determine the exact HfO_2 thickness. The interfacial roughness was not an imaging artifact because the Si lattice was visible, the Si/SiO_2 interface abrupt and both showed uniform contrast. The roughening/interdiffusion was more severe at the top (TiN) interface and caused an overlap of the HfO_2 and the TiN grains along the direction of the electron beam. The length scale of the roughening was smaller than the average HfO_2 grain size (note that Fig. 1(b) shows a single HfO_2 grain). Roughening may be due to reaction, intermixing or instability of the interface plane. Ti $L_{2,3}$ - fine structures in EELS (not shown) of the overlapping regions resembled those in TiN, with no crystal field splitting as expected for TiO_2. However, other oxides of Ti were more difficult to distinguish. Thus, the driving force for the roughening/interdiffusion at this interface is poorly understood.

To further investigate the roughening of the bottom interface, Fig. 2 shows a higher magnification HAADF image of this interface in the 900 °C annealed stack and line intensity profiles taken from different regions. Along this interface, HAADF images showed clusters of bright intensity within the SiO_2-like layer (circled in Fig. 2), which indicated the presence of heavy Hf clusters. These Hf clusters were found protruding from the HfO_2 layer, whereas no Hf clusters were observed next to the Si. Similar observations have been reported by others [12]. Clusters appeared to be at least several nm spaced apart, but this may also be due to limited sensitivity of this method to atoms located at greater depth along the beam direction in an amorphous matrix [13]. An intensity profile [Fig. 2(b)] showed that the intensity attributed to Hf

clusters was significantly above the background noise in the SiO_2-like layer. Figure 2 (c) shows intensity profiles across the SiO_2/HfO_2 interface. The profile along line 2 in Fig. 2(a) showed that the change in intensity at the interface was not a step function, which was due to interfacial roughness convoluted with the finite probe width [11]. The profile along line 3 exhibited an additional shoulder due to presence of heavy Hf clusters (arrow in Fig. 2(c)).

To investigate changes in the electronic structure of HfO_2 films as a function of annealing temperature, low-loss EELS spectra were recorded from the center of the HfO_2 films and from the HfO_2 reference powder (Fig. 3). In the reference HfO_2, the energy-losses of the peaks (in eV) were ~ 5.6 (A), ~ 15.5 (B), ~ 19 (C), ~ 26.6 (D), 35 (E), ~ 37 (F), ~ 42 (G), and ~ 47 eV (H). The low-loss EELS of the HfO_2 films showed no additional features; therefore the signal originated from the HfO_2 film only.

Low-loss energy loss features (< 30 eV) have been investigated by several authors for the chemically and structurally similar ZrO_2 [14-18]. Peak A corresponded to the energy of the optical band gap (~ 5.6 – 5.8 eV [19,20]), whereas feature at higher energy losses (peaks E-H) were due to the Hf O-edge. Some debate exists in the literature as to which of the strong peaks (B and/or D) corresponds to the plasmon excitation. Due to its strength in the as-deposited sample, and the fact that it shifted to higher energy losses with increasing annealing temperatures, we assigned peak D to a plasmon excitation. With this assignment, peak B was either a plasmon peak [17] or a single electron interband transition between O 2p and Hf 5d [15]. The difference in the plasmon energy (D) of almost 2 eV between the HfO_2 reference sample and the as-deposited film could be explained with the low intensity of B in the films. For example, interband transitions below plasmon peaks shift the plasmon to higher energies [21].

With higher anneal temperatures, the low-loss EELS more closely resembled that of the reference HfO_2. Specifically, Peak A was only visible for samples annealed above 800 °C. The absence of a sharp onset at the band edge for the film annealed at lower temperatures was likely due to a combination of the relatively low intensity of this feature even in the reference sample and states below the conduction band for films annealed at 700 °C. In addition to the shift described above, the plasmon peak was much broader in the films, indicating that defects caused greater damping through scattering with the lattice than in bulk HfO_2. The Hf O-edge (peaks E-H) was difficult to detect in the as-deposited sample, but sharpened with increasing annealing temperatures. Broadening of core-loss excitations is caused by a variation of bond angles, lengths and coordination due to strain or nonstoichiometry. The samples were crystallized, i.e. annealing temperatures were sufficient for atoms to be mobile, but apparently did not produce defect-free films. Broadening of EELS O K core-loss edges of ALD HfO_2 films annealed at temperatures below 850 °C was also observed by Wilk et al., who explained this with the presence of oxygen vacancies [9]. In contrast, the observed densification of the HfO_2 films upon high-temperature processing in this study was more likely correlated with the removal of excess oxygen or hydroxyl from the films with annealing, resulting in changes in the electronic structure. Alternative explanations included the removal of unintentional impurities or other point defects with annealing.

The most important observation from low-loss EELS was the significant change in the electronic structure that occurred upon annealing at 700 °C with the TiN electrode, even though the as-deposited stack had been exposed to *the same temperature* (700 °C) before TiN deposition. For example, note that peak B was hardly visible in the "as-deposited" film, whereas

it is visible in the film annealed with TiN. This result indicated that the TiN electrode acted as a sink for impurities or excess oxygen, similar to what was observed for Ti electrodes [22].

In summary, crystalline HfO_2 films exposed to relative high temperatures did not possess bulk electronic structure, as exhibited by the broadening of interband and core-loss transitions and the absence of a sharp onset at the band edge. Annealing to higher temperatures caused the electronic structure to more closely resemble that of bulk HfO_2, although features were still broader in the films. Changes in the point defect chemistry were likely responsible for a more bulk-like electronic structure in films annealed at higher temperatures. In particular, annealing with the TiN electrode improved the electronic structure. High-temperature processing was, however, accompanied by roughening of both bottom (substrate) and top (electrode) interface. At the bottom interface, clusters of Hf atoms were found to protrude into the interfacial SiO_2 layer, possibly increasing the apparent permittivity of this interfacial layer compared to a pure, smooth SiO_2 layer. No Hf was found near the Si substrate within the detection limit of HAADF, so Hf apparently did not rapidly diffuse into the SiO_2.

M.P.A. thanks Drs. Dmitri Klenov and Steffen Schmidt for help with the microscope operation and SRCEA/Intel for a fellowship. This research was supported by SRC.

REFERENCES

[1] R. Chau, S. Datta, M. Doczy, B. Doyle, J. Kavalieros, and M. Metz, IEEE Electron Dev. Lett. **25,** 408-410 (2004).

[2] J. K. Schaeffer, S. B. Samavedam, D. C. Gilmer, V. Dhandapani, P. J. Tobin, J. Mogab, B.-Y. Nguyen, B. E. White, S. Dakshina-Murthy, R. S. Rai, Z.-X. Jiang, R. Martin, M. V. Raymond, M. Zavala, L. B. La, J. A. Smith, R. Garcia, D. Roan, M. Kottke, and R. B. Gregory, J. Vac. Sci. & Technol. B **21,** 11-17 (2003).

[3] J. Westlinder, T. Schram, L. Pantisano, E. Cartier, A. Kerber, G. S. Lujan, J. Olsson, and G. Groeseneken, IEEE Electron Dev. Lett. **24,** 550-552 (2003).

[4] P. S. Lysaght, J. J. Peterson, B. Foran, C. D. Young, G. Bersuker, and H. R. Huff, Mater. Sci. Semicond. Proc. **7,** 259-263 (2004).

[5] S. Sayan, S. Aravamudhan, B. W. Busch, W. H. Schulte, F. Cosandey, G. D. Wilk, T. Gustafsson, and E. Garfunkel, J. Vac. Sci. & Technol. A **20,** 507-512 (2002).

[6] D. Chi and P. C. McIntyre, Appl. Phys. Lett. **85,** 4699-4701 (2004).

[7] Y.-S. Lin, R. Puthenkovilakam, J. P. Chang, C. Bouldin, I. Levin, N. V. Nguyen, J. Ehrstein, Y. Sun, P. Pianetta, T. Conrad, W. Vandervorst, V. Venturo, and S. Selbrede, J. Appl. Phys. **93,** 5945-5952 (2003).

[8] M. Copel, M. C. Reuter, and P. Jamison, Appl. Phys. Lett. **85,** 458-460 (2004).

[9] G. D. Wilk and D. A. Muller, Appl. Phys. Lett. **83,** 3984-3986 (2003).

[10] M. Meuris, P. W. Mertens, A. Opdebeeck, H. F. Schmidt, M. Depas, G. Vereecke, M. M. Heyns, and A. Philipossian, Solid State Technol. **38,** 109 (1995).

[11] A. C. Diebold, B. Foran, C. Kisielowski, D. A. Muller, S. J. Pennycook, E. Principe, and S. Stemmer, Microsc. Microanal. **9,** 493-508 (2003).

[12] K. v. Benthem, M. Y. Kim, and S. J. Pennycook, Materials Research Society Fall Meeting (2004).

[13] P. M. Voyles, D. A. Muller, and E. J. Kirkland, Microsc. Microanal. **10,** 291-300 (2004).

[14] J. Frandon, B. Brousseau, and F. Pradal, Phys. Stat. Sol. B **98,** 379-385 (1980).

[15] S. Kobayashi, A. Yamasaki, and T. Fujiwara, Jap. J. Appl. Phys. Part 1 **42,** 6946-6950 (2003).

[16] P. Prieto, F. Yubero, E. Elizalde, and J. M. Sanz, J. Vac. Sci. & Technol. A **14,** 3181-3188 (1996).

[17] D. W. McComb, Phys. Rev. B **54,** 7094-7102 (1996).

[18] L. K. Dash, N. Vast, P. Baranek, M. C. Cheynet, and L. Reining, Phys. Rev. B **70** (2004).

[19] S. G. Lim, S. Kriventsov, T. N. Jackson, J. H. Haeni, D. G. Schlom, A. M. Balbashov, R. Uecker, P. Reiche, J. L. Freeouf, and G. Lucovsky, J. Appl. Phys. **91,** 4500-4505 (2002).

[20] N. I. Medvedeva, V. P. Zhukov, M. Y. Khodos, and V. A. Gubanov, Phys. Stat. Sol. B **160,** 517-527 (1990).

[21] R. F. Egerton, *Electron Energy-Loss Spectroscopy in the Electron Microscope*, second ed. (Plenum Press, New York, 1996).

[22] H. Kim, P. C. McIntyre, C. O. Chui, K. Saraswat, and S. Stemmer, J. Appl. Phys. **96,** 3467–3472 (2004).

FIGURES

Figure 1 (color online)

HAADF images of the (a) the 800 °C and (b) 900 °C annealed samples. The dashed lines are a guide to the eye to indicate the approximate position of the interfacial layer. Note the roughening of interfaces after the 900 °C anneal.

Figure 2 (color online)

(a) High-resolution HAADF image of the lower interface of the 900°C stack and location of the line intensity profiles shown in (b-c). The inset shows a magnified portion of the image with different brightness/contrast settings to show the Hf clusters (circled). (b) Intensity profile along line 1 in (a). (c) Intensity profiles along lines 2 and 3 in (a).

Figure 3 (color online)

Low-loss EELS recorded from the middle of the HfO_2 films annealed at different temperatures and from the HfO_2 reference powder. Significant peaks are labeled A-H.

Figure 1

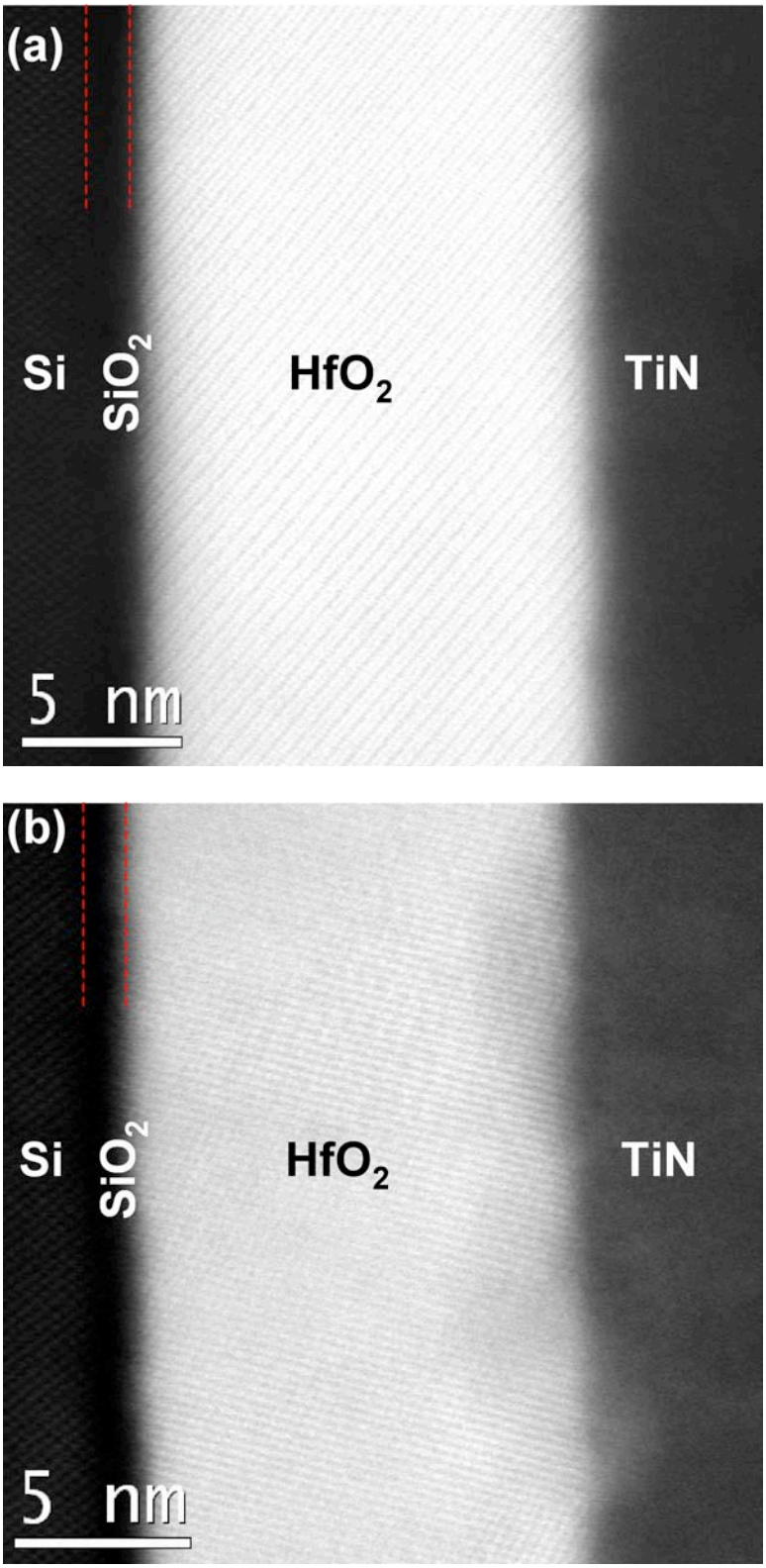

Figure 2

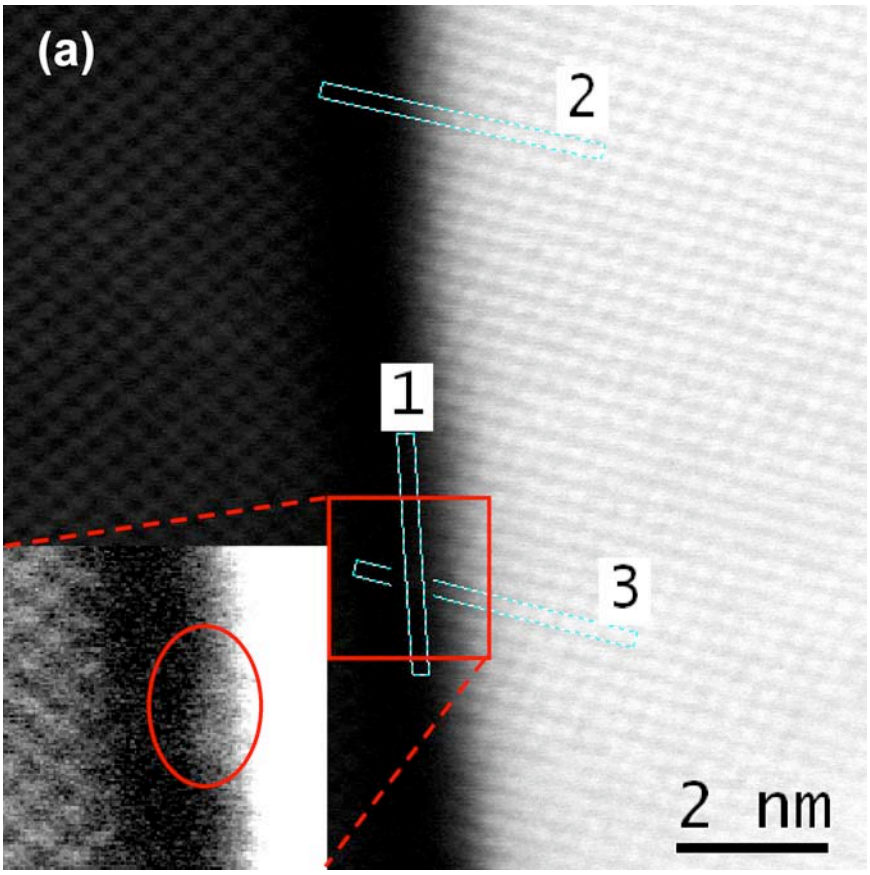
(a)
2
1
3
2 nm

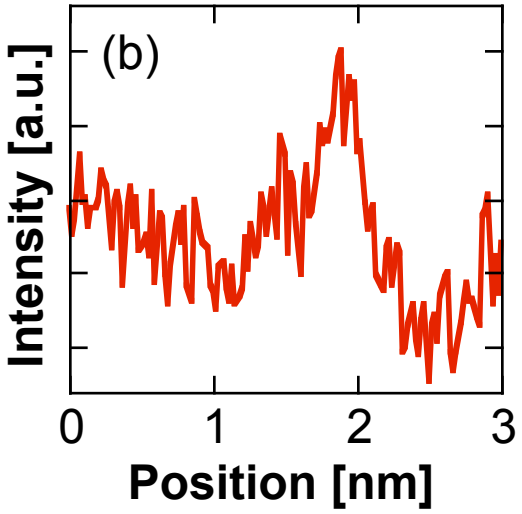
(b)
Intensity [a.u.]
0
1
2
3
Position [nm]

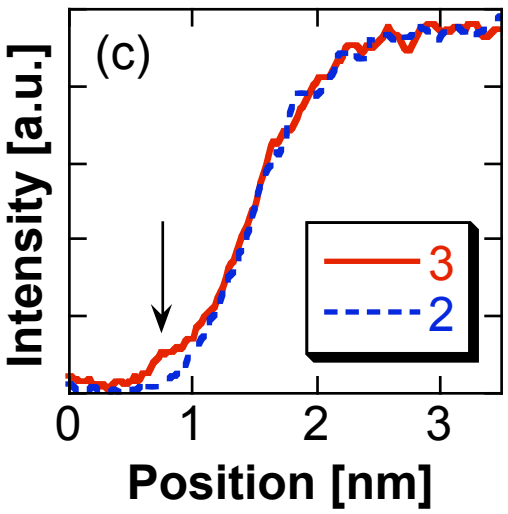
(c)
Intensity [a.u.]
3
2
0
1
2
3
Position [nm]

Figure 3

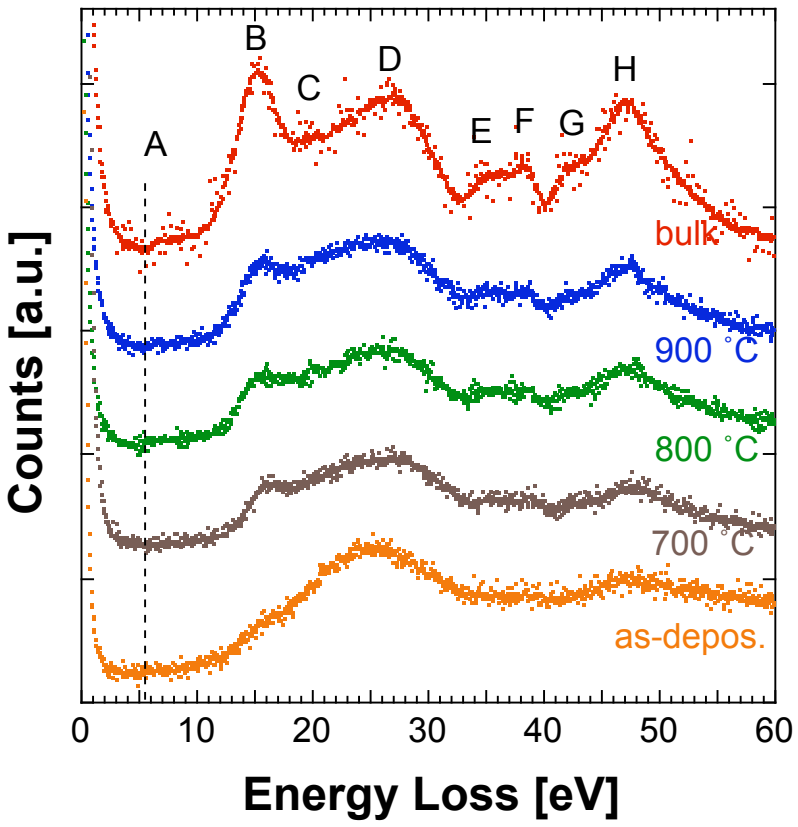
A
B
C
D
E
F
G
H
bulk
900 ˚C
800 ˚C
700 ˚C
as-depos.
Counts [a.u.]
0
10
20
30
40
50
60
Energy Loss [eV]